

Breaking the paradigm: record quindecim charged magnetic ionic liquids

Denis Prodius,^a Volodymyr Smetana,^a Simon Steinberg,^{a,b,c} Magdalena Wilk-Kozubek,^{a,b}

Yaroslav Mudryk,^a Vitalij K. Pecharsky,^{a,b} Anja-Verena Mudring^{*,a,b}

^aAmes Laboratory, US Department of Energy and Critical Materials Institute, Ames, Iowa 50011-3020, USA

^bDepartment of Materials Sciences and Engineering, Iowa State University, Ames, Iowa 50011-1096, USA

^c (present address): Institute of Inorganic Chemistry, RWTH-Aachen University, Aachen, Germany

*Corresponding author: Prof. Dr. Anja-Verena Mudring <mudring@iastate.edu>

Supplementary Information

Table of content

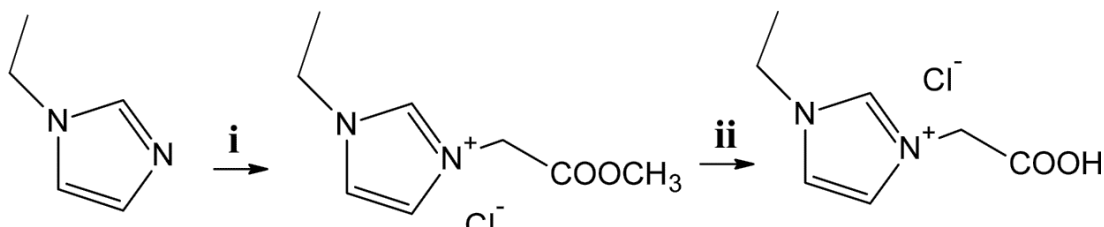
1.	Synthesis	S2
2.	X-ray analysis	S4
3.	Thermal Characterization	S7
4.	Infrared spectra	S9
5.	Mass spectral data for 1-3 (positive ion mode)	S10
6.	Supplementary Figures (magnetic properties)	S12
7.	NMR Spectra	S14
8.	Catalyst Evaluation (Tables S6-S7)	S15
9.	Photoluminescence properties	S15

1. Synthesis

The chemicals (1-ethylimidazolium, methyl chloroacetate) were of ACS reagent grade (>99%, *Sigma-Aldrich*) and used as received. All products were analyzed by CHN elemental analysis (Elementar Vario EL Analyzer, Hanau, Germany) and infrared spectroscopy (Agilent Cary 630 FTIR Spectrometer, Santa Clara, California, USA).

$[C_2H_5\text{-Im-CH}_2\text{-COOH}]Cl$ (**L1**):

1-carboxymethyl-3-ethylimidazolium chloride, $[C_2H_5\text{-Im-CH}_2\text{-COOH}]Cl$, has been obtained according to the Scheme S1 as described in [S1]:



Scheme S1: Synthesis of 1-carboxymethyl-3-ethylimidazolium chloride. Reagents and conditions: (i) 1 eq. $ClCH_2COOCH_3$, RT, 1.5 h; (ii) 37% aqueous HCl solution, 100 °C, 3 h.

Anal. calc. for $C_7H_{11}N_2Cl_1O_2$ (**L1**): C, 44.10; H, 5.82; N, 14.69; Found: C, 44.07; H, 5.80; N, 14.66. IR, cm^{-1} : 3431 (s, vb), 3108 (ms, sh), 3068 (s), 3003 (w), 2983 (w), 2712 (w), 2601 (w), 2514 (m), 2429 (mw), 1732 (s, b), 1641 (w, b), 1562 (m), 1466 (w), 1449 (w), 1435 (w), 1407 (s), 1362 (w), 1305 (w), 1229 (s), 1166 (s), 1082 (w), 1028 (w), 980 (w), 951 (w), 898 (m), 876 (m), 804 (w), 780 (m), 757 (mw), 676 (m, sh), 652 (s), 623 (w), 405 (w); Yield: ~98%.

[S1] D. Prodius, F. Macaev, Y. Lan, G. Novitchi, S. Pogrebnoi, E. Stingaci, V. Mereacre, C. E. Anson and A. K. Powell, *Chem. Comm.* **2013**, *49*, 9215-9217.

$[Ln_5(C_2H_5\text{-C}_3H_3N_2\text{-CH}_2COO)]_{16}(H_2O)_8](Tf_2N)_5$

To obtain $[Ln_5(C_2H_5\text{-C}_3H_3N_2\text{-CH}_2COO)]_{16}(H_2O)_8](Tf_2N)_5$, a mixture of 10 mmol of the respective lanthanide sesquioxide and 1-carboxymethyl-3-ethylimidazolium chloride (11.438 g, 60 mmol) was stirred in 100 ml of water under reflux for 24 hours. Solid $Li[Tf_2N]$ (17.22 g, 60 mmol) was added to the hot solution and the reaction mixture stirred for additional 30 min. After cooling to room temperature, a hydrophobic phase separated at the bottom of the reaction container. The supernatant aqueous liquid was decanted. Over a period of a few days further phase separation occurs. When this process was completed, the ionic liquid was separated by decantation, washed with 40 ml of water at RT. Finally, the product was separated using a separatory funnel as pink hydrophobic liquid (Figure S1a), heated at 100 °C for 5 hours and left for crystallization in a Petri dish (D x H = 150 x 15 mm; ambient conditions). Single crystals of (**1**) of sufficient quality for single crystal X-ray diffraction analysis can be collected after a period of 3-4 months (Figure S1b).



Figure S1: Freshly obtained compound **1** in the metastable liquid form (a) and single crystals collected after six month of crystallization time (b).

[Er₅(C₂H₅-C₃H₃N₂-CH₂COO)₁₆(H₂O)₈](Tf₂N)₁₅ (1):

Anal. calc. for C₁₄₂H₁₇₆N₄₇F₉₀S₃₀O₁₀₀Er₅ (**1**): C, 22.30; H, 2.32; N, 8.61; Found: C, 22.17; H, 2.30; N, 8.47. IR, cm⁻¹: 3502 (b, w), 3145 (b, w), 2959 (b, w), 1625 (b, m), 1568 (w), 1453 (sh, m), 1409 (sh, m) 1342 (s), 1323 (s), 1181 (sh, vs), 1129 (sh, vs), 1047 (sh, vs), 976 (w), 835 (b, w), 790 (sh, m), 742 (sh, m), 690 (m-w), 652 (sh, m); Yield: ~73% (22.34 g).

[Ho₅(C₂H₅-C₃H₃N₂-CH₂COO)₁₆(H₂O)₈](Tf₂N)₁₅ (2):

Anal. calc. for C₁₄₂H₁₇₆N₄₇F₉₀S₃₀O₁₀₀Ho₅ (**2**): C, 22.33; H, 2.32; N, 8.62; Found: C, 22.21; H, 2.28; N, 8.51. IR, cm⁻¹: 3502 (b, w), 3145 (b, w), 2959 (b, w), 1610 (b, m), 1565 (w), 1420 (sh, m), 1409 (sh, m) 1342 (s), 1319 (s), 1181 (sh, vs), 1129 (sh, vs), 1051 (sh, vs), 976 (w), 835 (b, w), 790 (sh, m), 742 (sh, m), 690 (w), 652 (sh, m); Yield: ~75% (22.95 g).



[Tm₅(C₂H₅-C₃H₃N₂-CH₂COO)₁₆(H₂O)₈](Tf₂N)₁₅ (3):

Anal. calc. for C₁₄₂H₁₇₆N₄₇F₉₀S₃₀O₁₀₀Tm₅ (**3**): C, 22.27; H, 2.32; N, 8.60; Found: C, 22.15; H, 2.34; N, 8.46. IR, cm⁻¹: 3502 (b, w), 3145 (b, w), 2959 (b, w), 1610 (b, m), 1565 (w), 1420 (sh, m), 1409 (sh, m) 1342 (s), 1319 (s), 1181 (sh, vs), 1133 (sh, vs), 1055 (sh, vs), 976 (w), 835 (b, w), 790 (sh, m), 742 (sh, m), 690 (m-w), 652 (m); Yield: ~78% (23.89 g).



Differential scanning calorimetry (DSC) was performed with a computer-controlled Phoenix DSC 204 F1 thermal analyser (Netzsch, Germany) with nitrogen as the protection gas. The samples were placed in aluminium pans. Experimental data is displayed in such a way that exothermic peaks occur at negative heat flow and endothermic peaks at positive heat flow. DSC runs included heating and subsequent cooling at 10°C/min. Given temperatures correspond to the onset of the respective thermal process. Thermogravimetric analyses were carried out in a dry air stream on a STA 449 F3 Jupiter (Netzsch, Germany) in sealed (pierced) aluminum pans.

Positive ion mode ESI mass spectra were obtained using the LCQ Advantage mass spectrometer. Equipped with a Surveyor Pump system and a Surveyor autosampler. 1 µL of sample (concentration of approximately 10 ppm) was injected into the LCQ Advantage ESI ion source. Water/MeOH (0.1% formic acid) 50/50 was used as effluent solvent. The mass range was kept constant from 100 to 1000 amu. The instrument was operated in the 4GHz HRes mode. Accurate mass measurement was achieved by constantly infusing a calibrant (masses: 121.0508 and 922.0098).

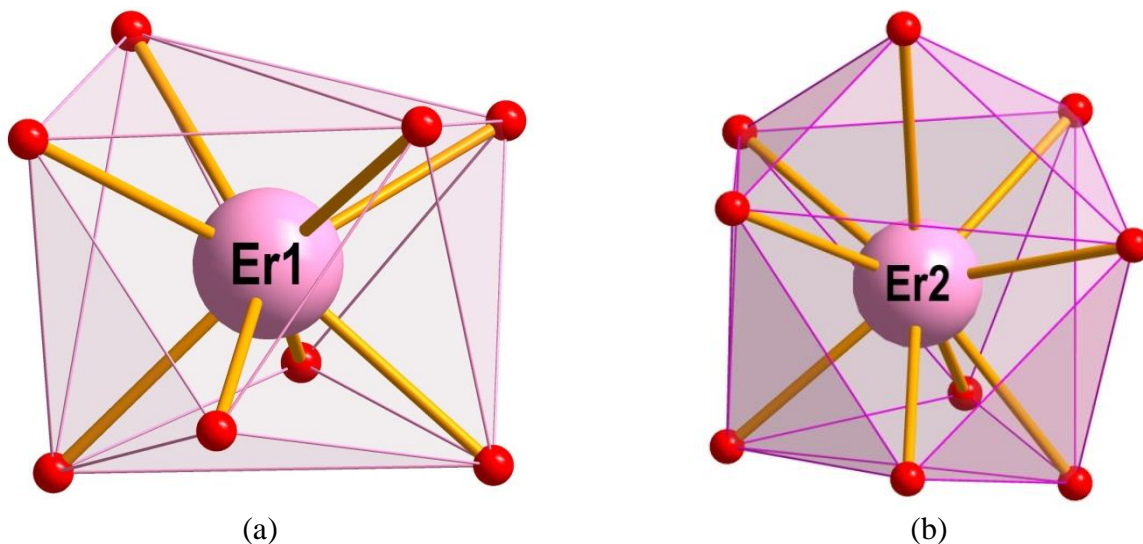


Figure S2: Views of two different coordination environments of Er in **1**: (a) square antiprismatic and axially capped square antiprismatic (b).

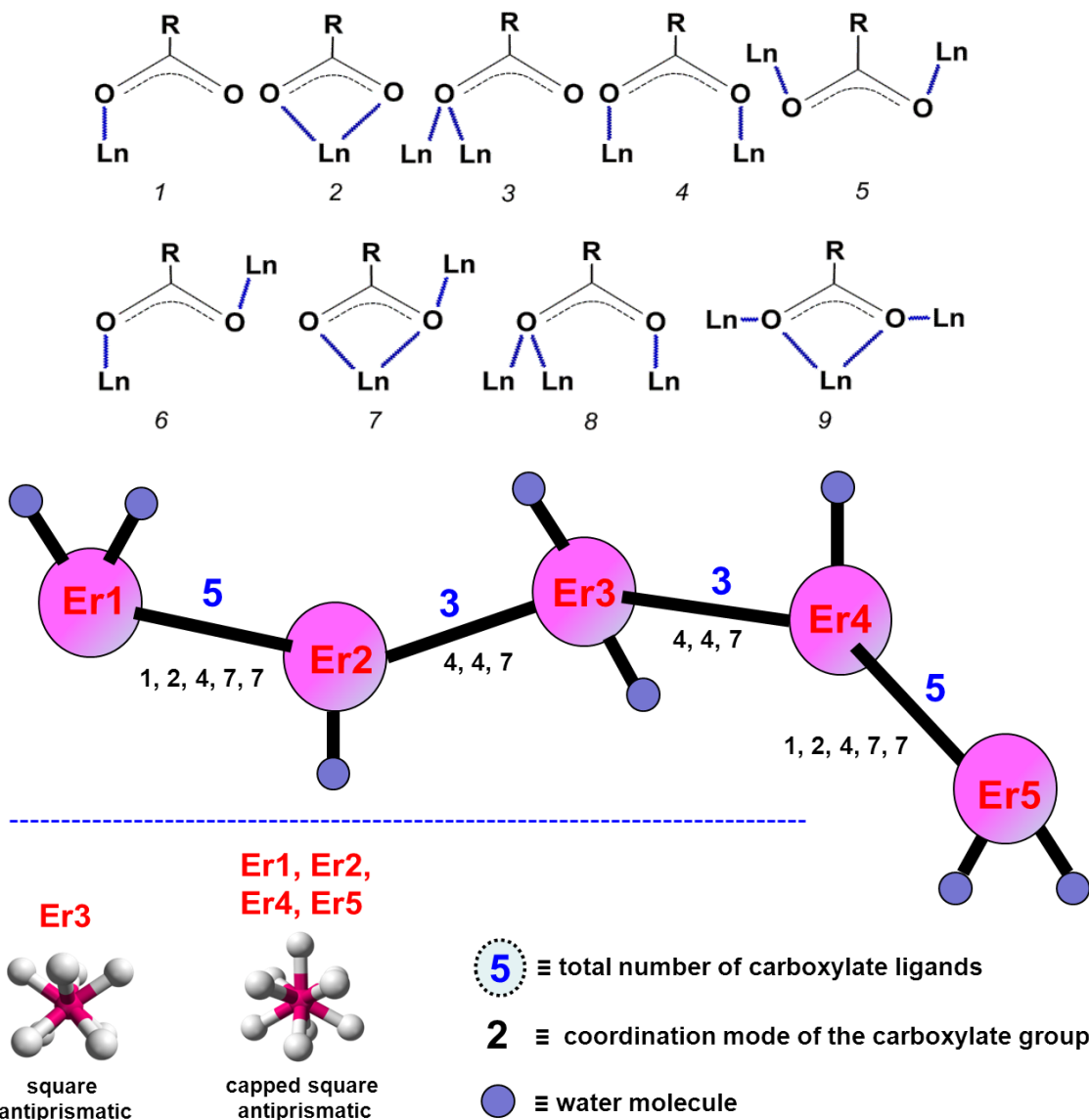


Figure S3: Common coordination modes of the carboxylate group found in rare earth carboxylates: η^1 (1); η^2 (2); $\eta^2 : \mu_2$ (3); $\eta^1 : \eta^1 : \mu_2\text{-ZZ}$ (4); $\eta^1 : \eta^1 : \mu_2\text{-EE}$ (5); $\eta^1 : \eta^1 : \mu_2\text{-ZE}$ (6); $\eta^2 : \eta^1 : \mu_2$ (7); $\eta^2 : \eta^1 : \mu_3$ (8); $\eta^2 : \eta^2 : \mu_3$ (9) (up); schematic structural representation of the pentanuclear cation in **1** (bottom).

Single crystal X-ray analysis has been performed on crystals with a size of $200\text{ }\mu\text{m}$ specimens selected from the bulk. Sets of single-crystal X-ray intensity data were collected at low temperature ($\sim 173\text{ K}$) with Mo-K α radiation (APEX CCD diffractometer Bruker Inc., Madison, USA, $\lambda = 0.71073\text{ \AA}$) in ϕ - and ω -scan modes with at least 2000 frames and exposures of 40 s per frame. The reflection intensities were integrated with the aid of the SAINT program of the SMART^[S2] software package over the entire reciprocal space. Empirical absorption corrections were accomplished using the program SADABS.^[S3] The XPREP algorithms in the SHELXTL software package were employed for analyzing the fulfilled reflection conditions pointing to the space group $Pca2_1$ (no. 29), which was used for the final refinement of the crystal structures. The starting atomic parameters derived via direct methods (SHELXS-97), while full-matrix least-square refinements on F^2 with anisotropic atomic displacement parameters were accomplished using the SHELXL-97 program.^[S4]

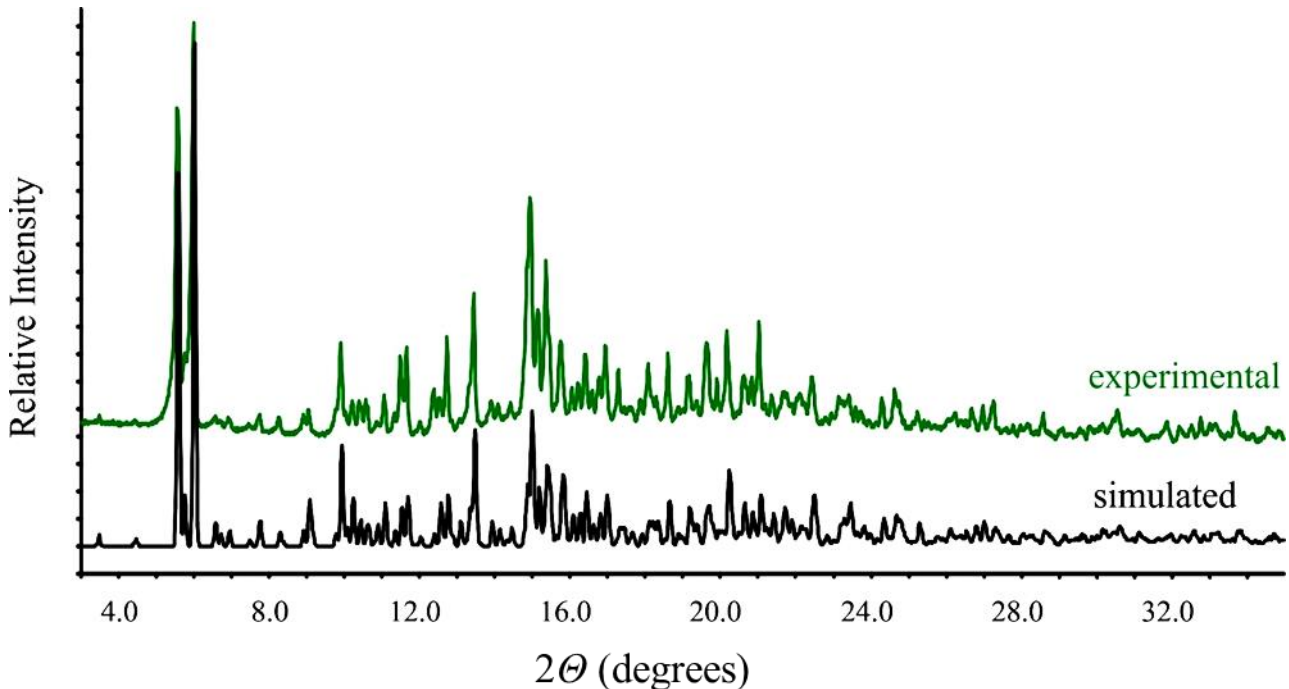
[S2] SMART: SMART, Bruker AXS, Inc.: Madison, WI, 1996.

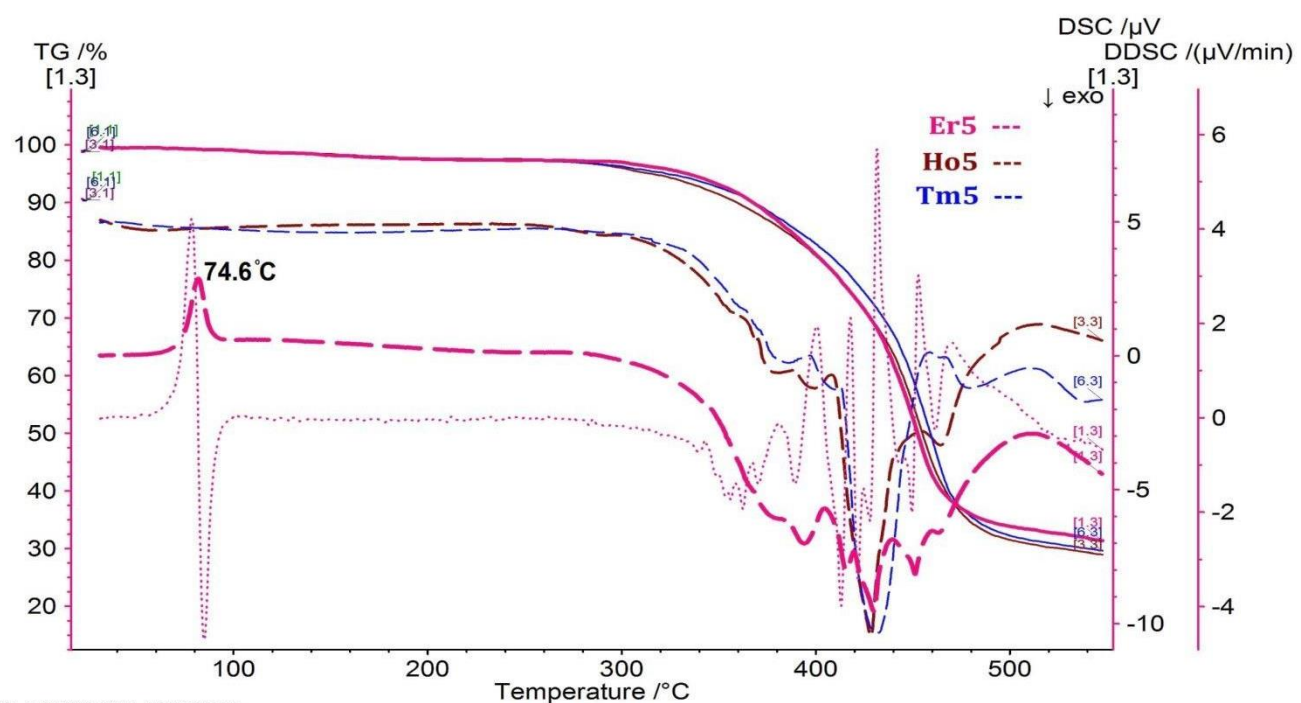
[S3] SADABS: Blessing, R., Acta Crystallogr., Sect. A 1995, 51, 33-38.

[S4] SHELX: Sheldrick, G. M., Acta Crystallogr., Sect. A 2008, 64, 112-122.

Table S1: Crystallographic data, details of data collection and structure refinement parameters for **1** and **2**.

	1	2
Empirical formula	C ₁₄₂ H ₁₇₆ N ₄₇ F ₉₀ S ₃₀ O ₁₀₀ Er ₅	
Formula weight	7649.388	
Temperature/K	173	173
Crystal system	orthorhombic	orthorhombic
Space group	Pca2 ₁	Pca2 ₁
<i>a</i> /Å	17.2096(2)	17.2652(5)
<i>b</i> /Å	31.3584(4)	31.3295(9)
<i>c</i> /Å	50.5444(6)	50.4955(13)
<i>V</i> /Å ³	27277.1(6)	27313.5(13)
<i>Z</i>	4	4
<i>F</i> 000	15084	
ρ_{calc} /g/cm ³	1.859	
μ /mm ⁻¹	1.906	
Crystal size/mm ³	0.20 × 0.20 × 0.20	
$\theta_{\min}, \theta_{\max}$ (°)	1.35 to 28.12	
Reflections collected	129635	
Independent reflections	56928 [$R_{\text{int}} = 0.0599$]	
Data/restraints/parameters	56928/44/3347	
GOF ^c	1.016	
$R_1^a (I > 2\sigma(I))$	0.0613	
$wR_2^b (\text{all data})$	0.1640	
Absolute structure parameter	0.286(8)	
Largest diff. peak/hole/e Å ⁻³	2.08/-1.30	

^a $R_1 = \sum ||F_o| - |F_c|| / \sum |F_o|$, ^b $wR_2 = \{\sum [w(F_o^2 - F_c^2)^2] / \sum [w(F_o^2)^2]\}^{1/2}$.^c GOF = $\{\sum [w(F_o^2 - F_c^2)^2] / (n - p)\}^{1/2}$, where *n* is the number of reflections and *p* is the total number of refined parameters**Figure S4:** Experimental and simulated powder X-ray diffraction pattern of {Er5} (**1**).

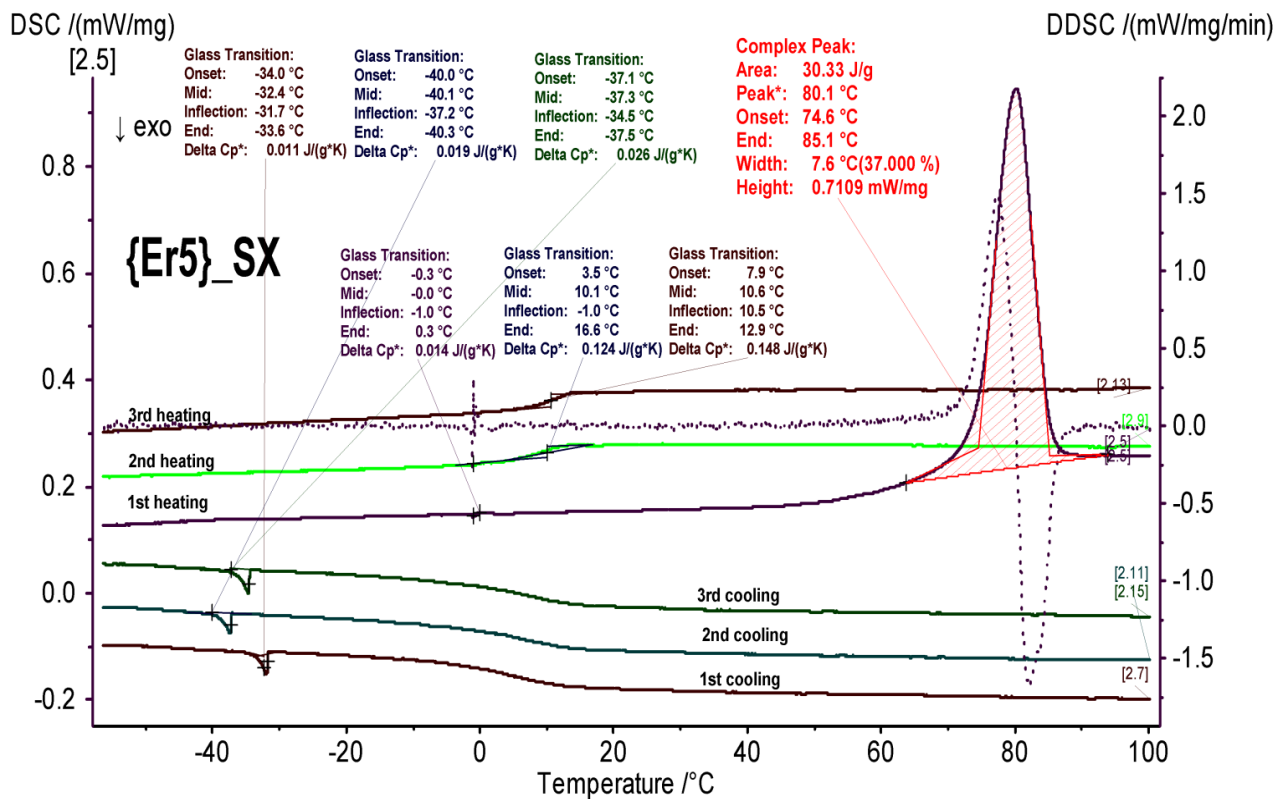


Main 2016-02-28 14:42 User: Cyclones

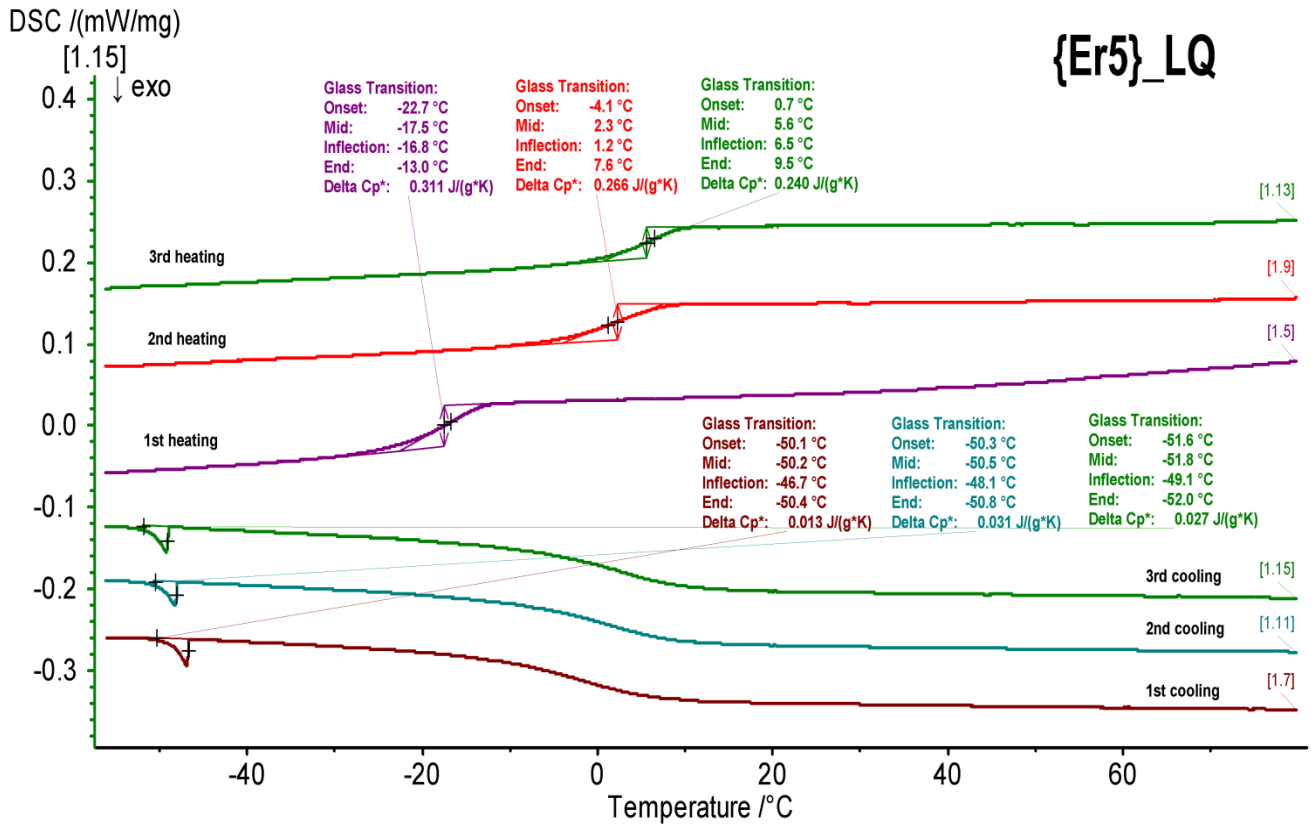
[#]	Instrument	File	Date	Identity	Sample	Mass/mg	Segment	Range	Atmosphere	Corr.
[1..1]	STA 449F3	Er5.ngb-ds3	2015-10-05	Er5	Er5	4.0	1/3	20°C/5.0(K/min)/30°C	N2/O2, 40.0ml/min / N2, 40.0ml/min	DSC:020, TG:020
[1..3]	STA 449F3	Er5.ngb-ds3	2015-10-05	Er5	Er5	4.0	3/3	30°C/10.0(K/min)/550°C	N2/O2, 40.0ml/min / N2, 40.0ml/min	DSC:020, TG:020
[3..1]	STA 449F3	Ho5.ngb-ds3	2015-10-07	Ho5	Ho5	3.9	1/3	20°C/5.0(K/min)/30°C	N2/O2, 40.0ml/min / N2, 40.0ml/min	DSC:020, TG:020
[3..3]	STA 449F3	Ho5.ngb-ds3	2015-10-07	Ho5	Ho5	3.9	3/3	30°C/10.0(K/min)/550°C	N2/O2, 40.0ml/min / N2, 40.0ml/min	DSC:020, TG:020
[6..1]	STA 449F3	Tm5a.ngb-ds3	2015-10-12	Tm5a	Tm5a	4.6	1/3	20°C/5.0(K/min)/30°C	N2/O2, 40.0ml/min / N2, 40.0ml/min	DSC:020, TG:020
[6..3]	STA 449F3	Tm5a.ngb-ds3	2015-10-12	Tm5a	Tm5a	4.6	3/3	30°C/10.0(K/min)/550°C	N2/O2, 40.0ml/min / N2, 40.0ml/min	DSC:020, TG:020

Created with NETZSCH Proteus software

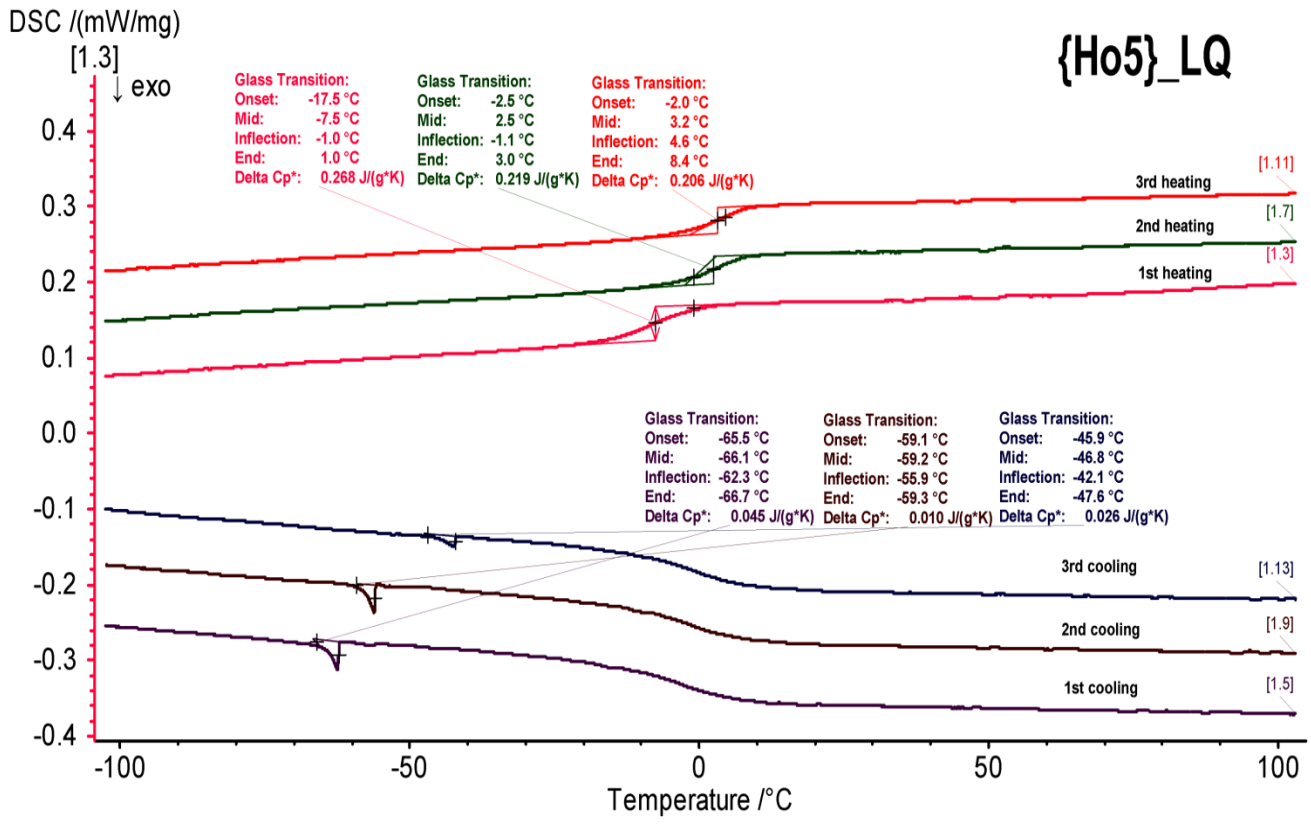
Figure S5: TG/DSC traces of the crystalline **1** and TG curves for liquid **2, 3** compounds at a heating rate of $10\text{ °C}\cdot\text{min}^{-1}$ under an air atmosphere.



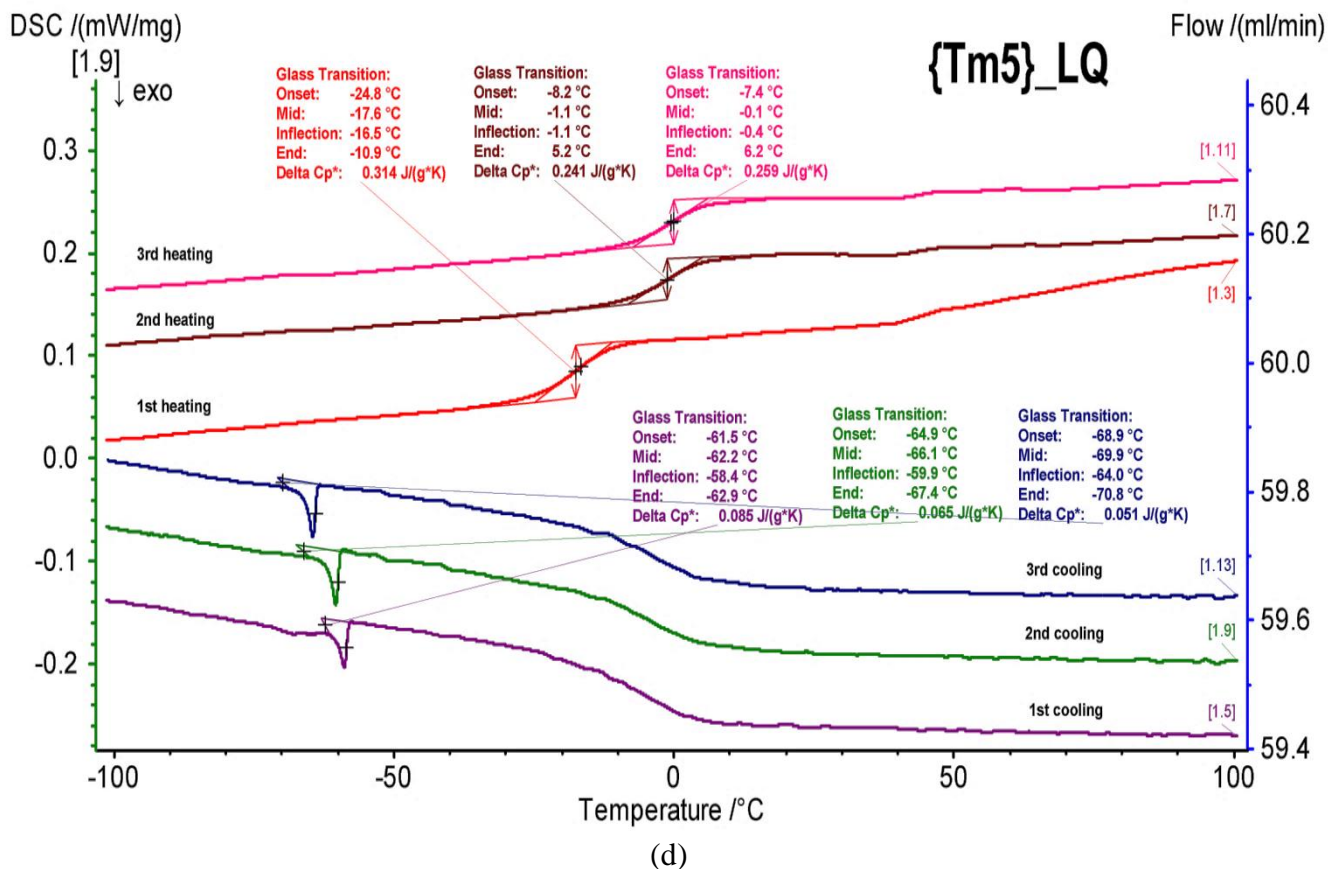
(a)



(b)



(c)



(d)

Figure S6: DSC thermograms of 1-3 with a scan rate of 10 °C/min and three thermal cycles for: a) $[Er_5(C_2H_5-C_3H_3N_2-CH_2COO)_{16}(H_2O)_8](Tf_2N)_{15}$ (as single crystals); b) $[Er_5(C_2H_5-C_3H_3N_2-CH_2COO)_{16}(H_2O)_8](Tf_2N)_{15}$ (liquid form); c) $[Ho_5(C_2H_5-C_3H_3N_2-CH_2COO)_{16}(H_2O)_8](Tf_2N)_{15}$ (liquid form); d) $[Tm_5(C_2H_5-C_3H_3N_2-CH_2COO)_{16}(H_2O)_8](Tf_2N)_{15}$ (liquid form).

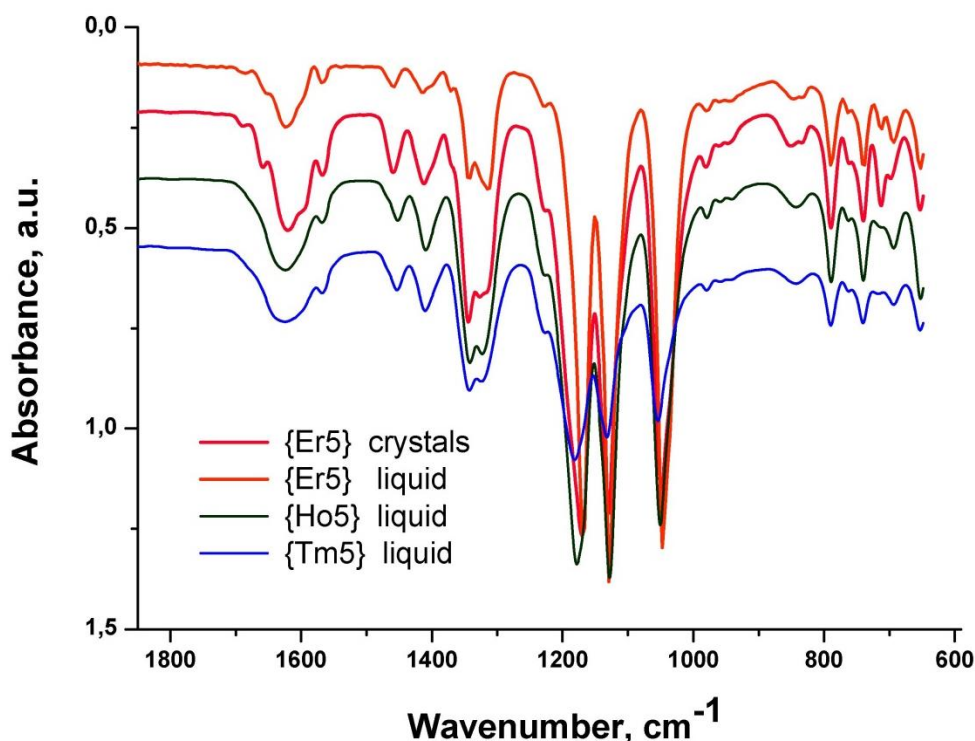


Figure S7: Infrared spectra of 1-3 in 1800-650 cm^{-1} region.

Table S2: Summary of phase transition temperatures, enthalpies and specific heat capacities for **1-3**.

Compound/ phase	Cycle	T _{onset} , °C				ΔH, J/g	ΔC _p (H), J/g·K	ΔC _p (C), J/g·K			
		Heating		Cooling							
		Glass transition (H)	Melting point	Glass transition (C)	Partial crystallization (C)			1	2		
								1	2		
{Ers} (1) solid	I	-0.3	74.6	11.2	-33.6	30.330	0.014	0.110	0.011		
	II	3.5	-	-4.9	-40.3	-	0.124	0.049	0.019		
	III	7.9	-	11.9	-37.5	-	0.148	0.166	0.026		
{Ers} (1) liquid	I	-22.7	-	5.7	-50.1	-	0.311	0.120	0.013		
	II	-4.1	-	7.8	-50.3	-	0.266	0.165	0.031		
	III	0.7	-	8.0	-51.6	-	0.240	0.152	0.027		
{Hos} (2) liquid	I	-17.5	-	14.3	-65.5	-	0.268	0.039	0.045		
	II	-2.5	-	-0.7	-59.1	-	0.219	0.120	0.010		
	III	-2.0	-	4.7	-45.9	-	0.206	0.139	0.026		
{Tms} (3) liquid	I	-24.8	-	3.4	-61.5	-	0.314	0.165	0.085		
	II	-8.2	-	-0.1	-64.9	-	0.241	0.106	0.065		
	III	-7.4	-	-13.3	-68.9	-	0.259	0.078	0.051		

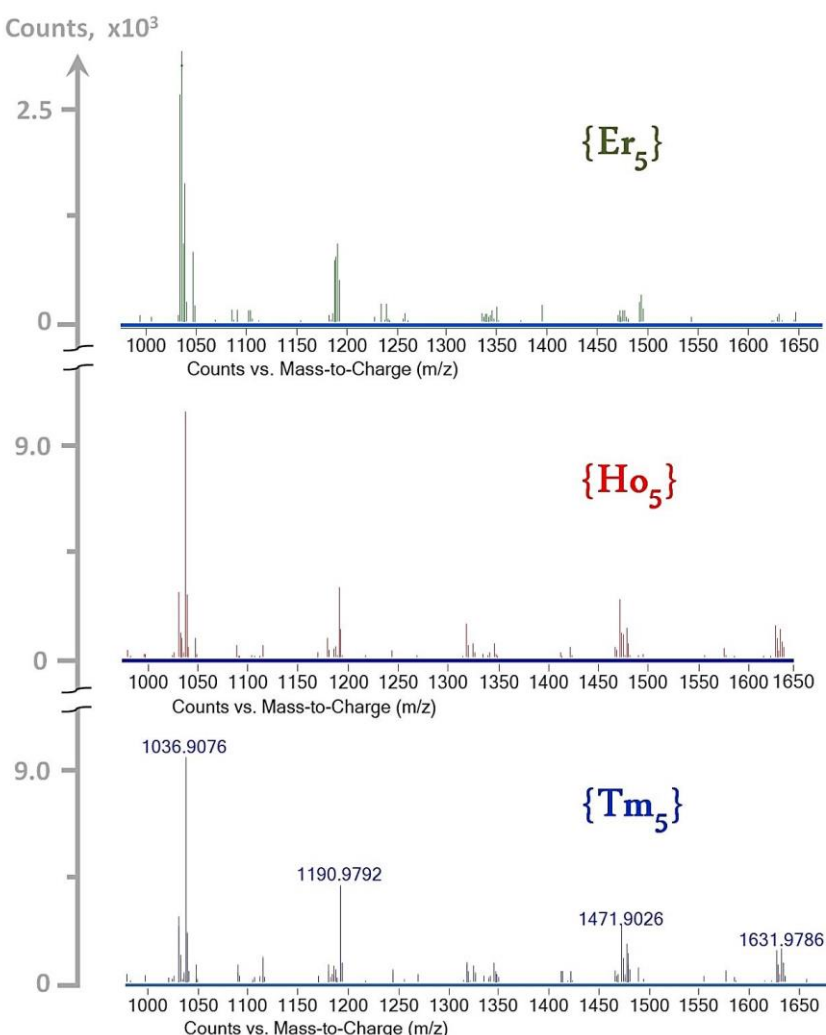
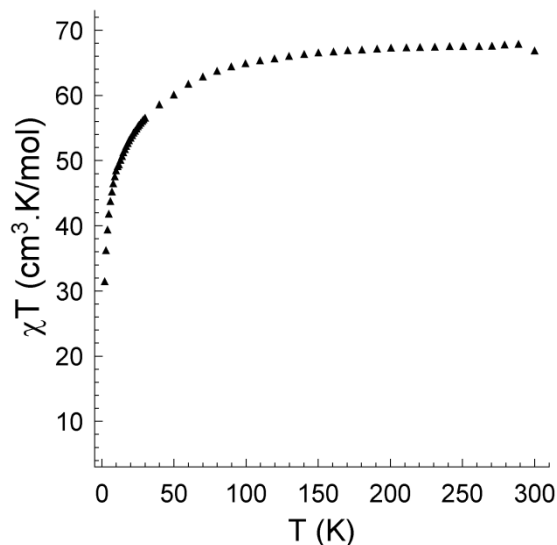


Figure S8: Fragment of ESI-MS (1000-1650, m/z) for compounds **1-3** in water.

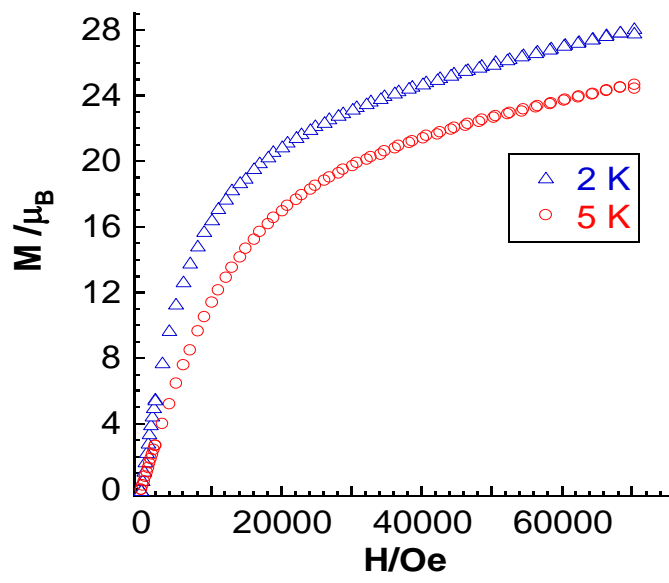
Table S3: Mass spectral data of selected peaks for **1-3** (positive ion mode).

	Formula	m/z	Fragment
1 [Er ₅ (C ₂ H ₅ -Im-CH ₂ COO) ₁₆ (H ₂ O) ₈](Tf ₂ N) ₁₅	155.0812	[C ₂ H ₅ -Im-CH ₂ COOH] ⁺	
	309.1539	[C ₂ H ₅ -Im-CH ₂ COOH...C ₂ H ₅ -Im-CH ₂ COO] ⁺	
	346.9978	[[(C ₂ H ₅ -Im-CH ₂ CO ₂ H)(C ₂ H ₅ -Im-CH ₂ CO ₂)(H ₂ O) ₂] ⁺	
	382.9977	[[(C ₂ H ₅ -Im-CH ₂ CO ₂ H)(C ₂ H ₅ -Im-CH ₂ CO ₂)(H ₂ O) ₄] ⁺	
	406.5485	[Er ₅ (C ₂ H ₅ -Im-CH ₂ COO) ₁₅ (H ₂ O) ₂ (Tf ₂ N) ₄] ¹¹⁺	
	455.0527	[Er ₅ (C ₂ H ₅ -Im-CH ₂ COO) ₁₅ (Tf ₂ N) ₅] ¹⁰⁺	
	524.8685	[Er ₅ (C ₂ H ₅ -Im-CH ₂ COO) ₁₄ (H ₂ O) ₂ (Tf ₂ N) ₆] ⁹⁺	
	590.0769	[(C ₂ H ₅ -Im-CH ₂ CO ₂ H) ₂ (Tf ₂ N)] ⁺	
	644.9145	[Er ₅ (C ₂ H ₅ -Im-CH ₂ COO) ₁₅ (H ₂ O) ₂ (Tf ₂ N) ₇] ⁸⁺	
	800.9894	[Er ₅ (C ₂ H ₅ -Im-CH ₂ COO) ₁₆ (H ₂ O) ₃ (Tf ₂ N) ₈] ⁷⁺	
	881.8335	[Er ₅ (C ₂ H ₅ -Im-CH ₂ COO) ₁₂ (H ₂ O) ₄ (Tf ₂ N) ₉] ⁶⁺	
	1035.9083	[Er ₅ (C ₂ H ₅ -Im-CH ₂ COO) ₉ (H ₂ O) ₈ (Tf ₂ N) ₁₀] ⁵⁺	
	1091.0168	[Er ₅ (C ₂ H ₅ -Im-CH ₂ COO) ₁₁ (H ₂ O) ₆ (Tf ₂ N) ₁₀] ⁵⁺	
	1189.9792	[Er ₅ (C ₂ H ₅ -Im-CH ₂ COO) ₁₄ (H ₂ O) ₈ (Tf ₂ N) ₁₀] ⁵⁺	
2 [Ho ₅ (C ₂ H ₅ -Im-CH ₂ COO) ₁₆ (H ₂ O) ₈](Tf ₂ N) ₁₅	1349.9597	[Er ₅ (C ₂ H ₅ -Im-CH ₂ COO) ₉ (H ₂ O) ₅ (Tf ₂ N) ₁₁] ⁴⁺	
	1492.8836	[Er ₅ (C ₂ H ₅ -Im-CH ₂ COO) ₁₃ (H ₂ O) ₂ (Tf ₂ N) ₁₁] ⁴⁺	
	1631.1612	[Er ₅ (C ₂ H ₅ -Im-CH ₂ COO) ₁₆ (H ₂ O) ₇ (Tf ₂ N) ₁₁] ⁴⁺	
	155.0823	[C ₂ H ₅ -Im-CH ₂ COOH] ⁺	
	309.1558	[C ₂ H ₅ -Im-CH ₂ COOH...C ₂ H ₅ -Im-CH ₂ COO] ⁺	
	346.9990	[(C ₂ H ₅ -Im-CH ₂ CO ₂ H)(C ₂ H ₅ -Im-CH ₂ CO ₂)(H ₂ O) ₂] ⁺	
	405.1496	[Ho ₅ (C ₂ H ₅ -Im-CH ₂ COO) ₁₅ (H ₂ O) ₂ (Tf ₂ N) ₄] ¹¹⁺	
	453.5350	[Ho ₅ (C ₂ H ₅ -Im-CH ₂ COO) ₁₅ (Tf ₂ N) ₅] ¹⁰⁺	
	521.8712	[Ho ₅ (C ₂ H ₅ -Im-CH ₂ COO) ₁₄ (H ₂ O)(Tf ₂ N) ₆] ⁹⁺	
	590.0782	[(C ₂ H ₅ -Im-CH ₂ CO ₂ H) ₂ (Tf ₂ N)] ⁺	
	643.9197	[Ho ₅ (C ₂ H ₅ -Im-CH ₂ COO) ₁₅ (H ₂ O) ₃ (Tf ₂ N) ₇] ⁸⁺	
	797.9928	[Ho ₅ (C ₂ H ₅ -Im-CH ₂ COO) ₁₆ (H ₂ O) ₃ (Tf ₂ N) ₈] ⁷⁺	
	878.8372	[Ho ₅ (C ₂ H ₅ -Im-CH ₂ COO) ₁₂ (H ₂ O) ₄ (Tf ₂ N) ₉] ⁶⁺	
	1032.9136	[Ho ₅ (C ₂ H ₅ -Im-CH ₂ COO) ₉ (H ₂ O) ₈ (Tf ₂ N) ₁₀] ⁵⁺	
	1109.9504	[Ho ₅ (C ₂ H ₅ -Im-CH ₂ COO) ₁₂ (H ₂ O) ₃ (Tf ₂ N) ₁₀] ⁵⁺	
	1186.9864	[Ho ₅ (C ₂ H ₅ -Im-CH ₂ COO) ₁₄ (H ₂ O) ₈ (Tf ₂ N) ₁₀] ⁵⁺	
3 [Tm ₅ (C ₂ H ₅ -Im-CH ₂ COO) ₁₆ (H ₂ O) ₈](Tf ₂ N) ₁₅	1341.0591	[Ho ₅ (C ₂ H ₅ -Im-CH ₂ COO) ₉ (H ₂ O) ₄ (Tf ₂ N) ₁₁] ⁴⁺	
	1489.0224	[Ho ₅ (C ₂ H ₅ -Im-CH ₂ COO) ₁₃ (H ₂ O) ₂ (Tf ₂ N) ₁₁] ⁴⁺	
	1614.1375	[Ho ₅ (C ₂ H ₅ -Im-CH ₂ COO) ₁₆ (H ₂ O) ₄ (Tf ₂ N) ₁₁] ⁴⁺	
	155.0816	[C ₂ H ₅ -Im-CH ₂ COOH] ⁺	
	309.1524	[C ₂ H ₅ -Im-CH ₂ COOH...C ₂ H ₅ -Im-CH ₂ COO] ⁺	
	346.1978	[(C ₂ H ₅ -Im-CH ₂ CO ₂ H)(C ₂ H ₅ -Im-CH ₂ CO ₂)(H ₂ O) ₂] ⁺	
	412.9994	[Tm ₅ (C ₂ H ₅ -Im-CH ₂ COO) ₁₆ (H ₂ O) ₅ (Tf ₂ N) ₄] ¹¹⁺	
	474.0661	[Tm ₅ (C ₂ H ₅ -Im-CH ₂ COO) ₁₆ (H ₂ O)(Tf ₂ N) ₅] ¹⁰⁺	
	533.0710	[Tm ₅ (C ₂ H ₅ -Im-CH ₂ COO) ₁₄ (H ₂ O) ₆ (Tf ₂ N) ₆] ⁹⁺	
	590.0763	[(C ₂ H ₅ -Im-CH ₂ CO ₂ H) ₂ (Tf ₂ N)] ⁺	
	647.9177	[Tm ₅ (C ₂ H ₅ -Im-CH ₂ COO) ₁₅ (H ₂ O) ₃ (Tf ₂ N) ₇] ⁸⁺	
	801.9900	[Tm ₅ (C ₂ H ₅ -Im-CH ₂ COO) ₁₆ (H ₂ O) ₃ (Tf ₂ N) ₈] ⁷⁺	
	882.8328	[Tm ₅ (C ₂ H ₅ -Im-CH ₂ COO) ₁₂ (H ₂ O) ₄ (Tf ₂ N) ₉] ⁶⁺	
	1036.9086	[Tm ₅ (C ₂ H ₅ -Im-CH ₂ COO) ₉ (H ₂ O) ₈ (Tf ₂ N) ₁₀] ⁵⁺	
	1113.9459	[Tm ₅ (C ₂ H ₅ -Im-CH ₂ COO) ₁₂ (H ₂ O) ₄ (Tf ₂ N) ₁₀] ⁵⁺	
	1190.9792	[Tm ₅ (C ₂ H ₅ -Im-CH ₂ COO) ₁₄ (H ₂ O) ₈ (Tf ₂ N) ₁₀] ⁵⁺	
	1345.0511	[Tm ₅ (C ₂ H ₅ -Im-CH ₂ COO) ₉ (H ₂ O) ₃ (Tf ₂ N) ₁₁] ⁴⁺	
	1471.9026	[Tm ₅ (C ₂ H ₅ -Im-CH ₂ COO) ₁₂ (H ₂ O) ₆ (Tf ₂ N) ₁₁] ⁴⁺	
	1631.9815	[Tm ₅ (C ₂ H ₅ -Im-CH ₂ COO) ₁₆ (H ₂ O) ₇ (Tf ₂ N) ₁₁] ⁴⁺	

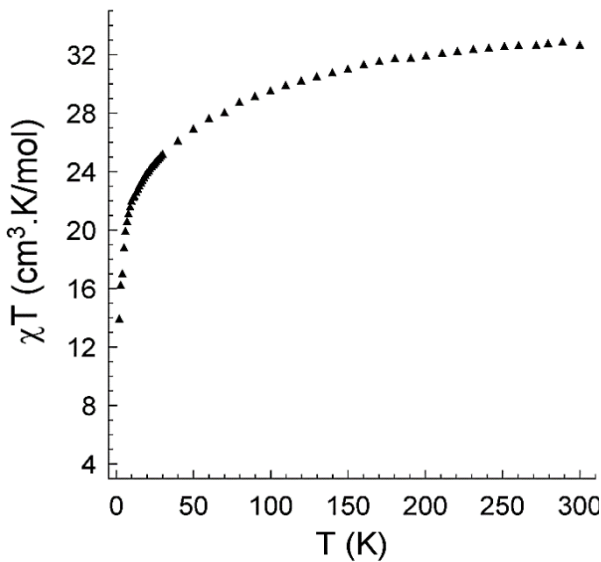
The DC magnetization was measured on a magnetic property measurement system MPMS (Quantum Design) as a function of both temperature (2–300 K range) and applied magnetic field.



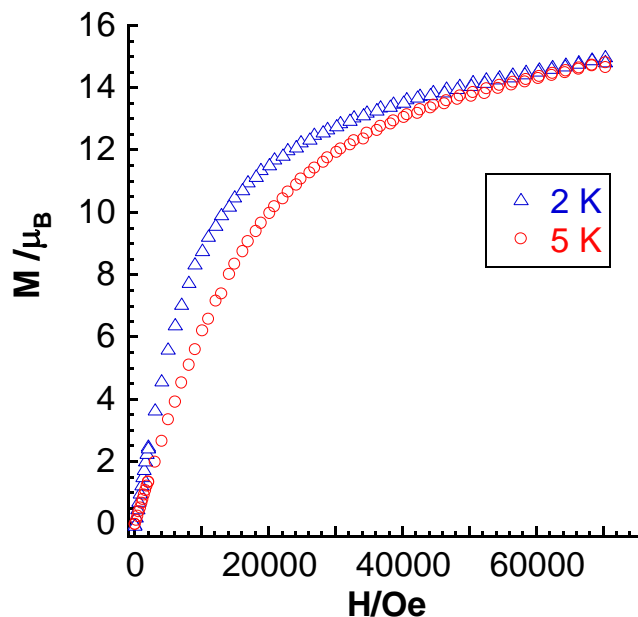
(a)



(b)



(c)



(d)

Figure S9: Plot of $\chi_M T$ vs T for compound **2** (a) and **3** (c) under 1000 Oe dc field and magnetisation (M) vs. applied field (H) for **2** (b) and **3** (d) at 2 and 5K.

Table S4: Selected magnetic data for **1-3**.

Compound	Ground state	Curie temperature, Θ (K)	calculated, $\mu_{\text{eff}} = g\sqrt{\vec{J}(\vec{J}+1)}$	experimental ^a μ_{Ln}	observed in literature ^{b, c}	experimental, ^d $\mu_{\text{eff}} = 2.83\sqrt{X_M T}$
{Er ₅ } (1)	⁴ I _{15/2}	-9.0	9.58	9.51	9.4-9.6	21.2
{Ho ₅ } (2)	⁵ I ₈	-6.0	10.61	10.50	10.4-10.7	23.3
{Tm ₅ } (3)	³ H ₆	-13.0	7.56	7.50	7.1-7.6	16.2

^a - effective moment per lanthanide ion; ^b C. Benelli, D. Gatteschi, "Introduction to Molecular Magnetism: From Transition Metals to Lanthanides, Wiley-VCH, Weinheim, 2015, pp.450; ^c - from http://www.radiochemistry.org/periodictable/la_series/L8.html; ^d - at RT, per pentanuclear unit.

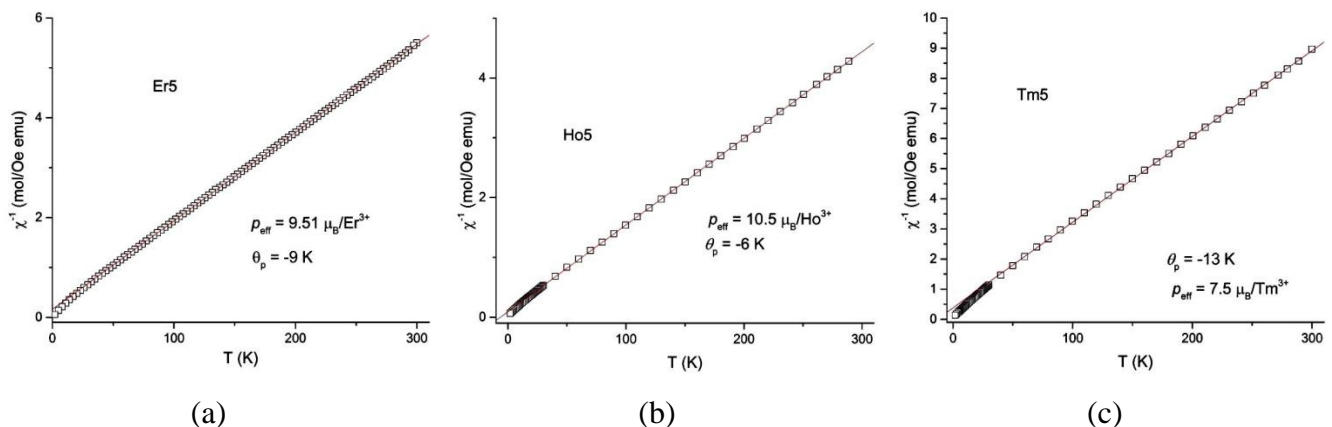


Figure S10: Temperature dependence of the reciprocal molar susceptibility for **1** (a), **2** (b) and **3** (c) at a field of 1000 Oe. The red line represents the best fitting to Curie-Weiss law.

Table S5: Comparative analysis (χT values) of some selected metal containing ionic liquids.

#	Compound	Number of metal atoms	Property	T _m , °C	χT measured at 300 K per complex (cm ³ K mol ⁻¹)	Ref.
1	{Er ₅ } (1)	5	paramagnetic	74.6/Liquid*	56.2	This work
2	{Ho ₅ } (2)	5	paramagnetic	Liquid*	67.9	This work
3	{Tm ₅ } (3)	5	paramagnetic	Liquid*	32.9	This work
4	{B-imS-C ₈ } [FeCl ₃ Br] ₃	3	paramagnetic	Liquid*	17.27	[1m]
5	{B-imS-C ₁₂ } [FeCl ₃ Br] ₃	3	paramagnetic	Liquid*	15.80	[1m]
6	[C ₆ mim] ₄ [Dy(SCN) ₇ (H ₂ O)]	1	paramagnetic	Liquid*	14.0±0.1	[2m]
7	[P ₆₆₆₁₄] ₃ DyCl ₆	1	paramagnetic	-47.7	12.9±0.6	[3m]
8	[P ₆₆₆₁₄] ₃ HoCl ₆	1	paramagnetic	-42.1	12.4±0.6	[3m]
9	{Dy-cmeim} (Tf ₂ N) ₃	1	Single Ion Magnet	Liquid*	11.6	[4m]
10	[P ₆₆₆₁₄] ₃ ErCl ₆	1	paramagnetic	-40.4	11.0±0.6	[3m]
11	{Fe ₃ -cmmim} (Tf ₂ N) ₇	3	antiferromagnetic interactions	92.0	10.4	[5m]
12	[C ₄ mim] ₂ [FeCl ₃ Br] ₂	2	paramagnetic	52.0	8.73	[6m]

* - liquid at RT

{B-imS-C₈} ≡ 1,3,5-tris(3-octyl-1-methyl-1*H*-imidazolium-1-yl)benzene; {B-imS-C₁₂} ≡ 1,3,5-tris(3-dodecyl-1-methyl-1*H*-imidazolium-1-yl)benzene; C₆mim ≡ 1-methyl-3-hexyl-imidazolium; P₆₆₆₁₄ ≡ tetradecyltrihexylphosphonium; cmeim ≡ 1-carboxymethyl-3-ethylimidazolium; cmmim ≡ 1-carboxymethyl-3-methylimidazolium; C₄mim₂ ≡ 1,1'-(1,2-ethyl)bis[3-butyl-1*H*-imidazolium-1-yl].

- [1m] Nacham, O.; Clark, K. D.; Yu, H.; Anderson, J. L.; Chem. Mater. 2015, 27, 923–931.
- [2m] Mallick, B.; Balke, B.; Felser, C.; Mudring, A.-V.; Angew. Chem. 2008, 120, 7747–7750; Angew. Chem. Int. Ed. 2008, 47, 7635–7638.
- [3m] Alvarez-Vicente, J.; Dandil, S.; Banerjee, D.; Gunaratne, H. Q. N.; Gray, S.; Felton, S.; Srinivasan, G.; Kaczmarek, A. M.; Van Deun, R.; Nockemann, P.; J. Phys. Chem. B 2016, 120, 5301–5311.
- [4m] Prodius, D.; Macaev, F.; Lan, Y.; Novitchi, G.; Pogrebnoi, S.; Stingaci, E.; Mereacre, V.; Anson, C. E.; Powell, A. K.; Chem. Commun. 2013, 49, 9215–9217.
- [5m] Prodius, D.; Macaev, F.; Lan, Y.; Novitchi, G.; Pogrebnoi, S.; Stingaci, E.; Mereacre, V.; Anson, C. E.; Powell, A. K.; Chem. Commun. 2013, 49, 9215–9217.
- [6m] Brown, P.; Butts, C.P.; Eastoe, J.; Hernandez, E.P.; Machado, F.L.A.; de Oliveira, R.J.; Chem. Commun., 2013, 49, 2765–2767.

General procedure for the synthesis of ethyl 2-methyl-4-(2-oxo-2,3-dihydro-1*H*-3-indolyl)-5-phenyl-1*H*-3-pyrrolecarboxylate

Ethyl 3-oxobutanoate (**4c**, 0.001 mol), **1-3** (1.31–1.36 μmol, Table S5) and ammonium acetate (**4b**, 0.0025 mol) was added to the suspension of 3-(2-oxo-2-phenylethylidene)indolin-2-one (**4a**, 0.001 mol) in dry EtOH (4 ml) at vigorously stirring. After 1 hour stirring under reflux the product was filtered off and the analytical sample was purified by recrystallization from EtOH.

Anal. calc. for C₂₂H₂₀N₂O₃ (**5**): C, 73.32; H, 5.59; N, 7.77. Found: C, 73.25; H, 5.54; N, 7.71. ¹H NMR (DMSO d-6, 400.13 MHz), δ, ppm, J/Hz: 0.86 t (3H, Me, J 8.0 Hz), 2.51 s (3H, Me), 3.73 q (2H, CH₂, J

8.0 Hz), 6.82-7.55 m (9H, arom), 10.34 s (1H, NH), 11.63 s (1H, NH). ^{13}C NMR (DMSO d-6, 100.61 MHz), δ , ppm: 178.9, 164.5, 143.4, 137.1, 132.3, 132.1, 129.3, 128.3, 128.2, 127.8, 127.4, 122.9, 121.3, 114.2, 110.2, 109.2, 58.3, 45.2, 14.4, 13.6.

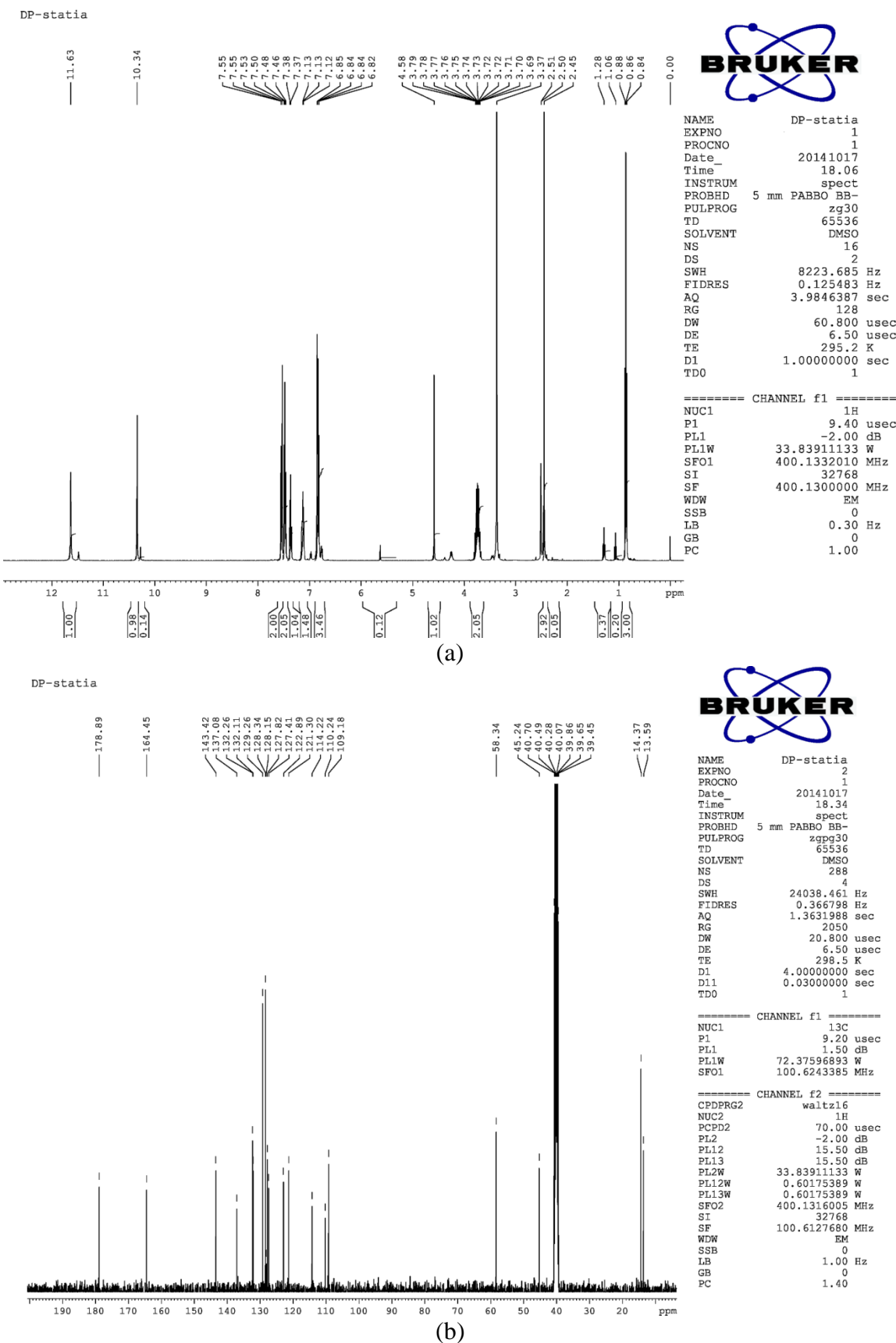


Figure S11: ^1H and ^{13}C NMR spectra of **5** in $(\text{CD}_3)_2\text{SO}$ at 400 MHz.

Table S6: The recycle of catalysts in synthesis of ethyl 2-methyl-4-(2-oxo-2,3-dihydro-1*H*-3-indolyl)-5-phenyl-1*H*-3-pyrrolecarboxylate (**5**).

Catalyst (mg, μmol)	MW, g/mol	Number of cycles/Yield [%]									
		1	2	3	4	5	6	7	8	9	10
1 (10.4, 1.360)	7649.35	98.3	97.2	94.4	95.8	95.0	94.4	91.6	90.2	88.8	86.1
2 (10.2, 1.335)	7637.70	97.6	96.6	94.1	93.5	92.8	91.6	91.0	90.1	88.9	87.5
3 (10.1, 1.312)	7657.72	95.4	94.6	93.0	90.8	88.3	88.8	86.1	86.4	85.9	85.0

Table S7: Catalytic activity of various catalysts on the three-component reaction of 2-pyrrolo-3-oxindoles.

#	Catalyst	mol%	Time (h)	Yield (%)	Yield (%) Run#6	Yield (%) Run#10	Ref.
1	{Er ₅ } (1)	0.029	1	98	94	86	This work
2	{Hos} (2)	0.030	1	97	92	88	This work
3	{Tm ₅ } (3)	0.029	1	95	89	85	This work
4	InCl ₃	20	0.25	92	-	-	[1p]
5	In(OTf) ₃	20	0.5	85	-	-	[1p]
6	BiCl ₃	20	1	60	-	-	[1p]
7	Bi(OTf) ₃	20	1	56	-	-	[1p]
8	[mcmmim]FeCl ₄	0.626	2	86	31	-	[2p]
9	{Fe ₃ -cmmim}{FeCl ₄) ₇	0.087	2	94	45	-	[2p]
10	{Fe ₃ -cmmim}{FeCl ₄) ₃ Cl ₄	0.147	2	98	90	62	[2p]
11	{Fe ₃ -cmmim}{Tf ₂ N) ₇	0.072	2	98	92	74	[2p]
12	{Fe ₃ -cepy}{FeCl ₄) ₆ Cl	0.091	2	96	88	73	[2p]

OTf \equiv CF₃SO₃⁻; mcmmim \equiv methyl 2-(3-methyl-1*H*-imidazol-1-yl)acetate; cmmim \equiv 1-carboxymethyl-3-methylimidazolium; cepry \equiv N-carboxyethylpyridinium.

[1p] Shanthi, G.; Perumal, R. T.; Tetrahedron Lett. 2009, 50, 3959–3962.

[2p] Prodius, D.; Macaev, F.; Lan, Y.; Novitchi, G.; Pogrebnoi, S.; Stingaci, E.; Mereacre, V.; Anson, C. E.; Powell, A. K.; Chem. Commun. 2013, 49, 9215–9217.

Near infrared luminescence measurements at room temperature

The corrected steady-state excitation and emission spectra were recorded on a HORIBA Jobin Yvon Fluorolog-3 spectrofluorometer, equipped with a 450 W xenon arc lamp and a Hamamatsu H10330B-75 NIR PMT detector. The decay curve measurements were performed on the same instrument, adapted for time-correlated single photon counting (TCSPC) measurements. A xenon flash lamp was used as the excitation source. Luminescence lifetimes were determined by tail-fitting the curves using a monoexponential model.

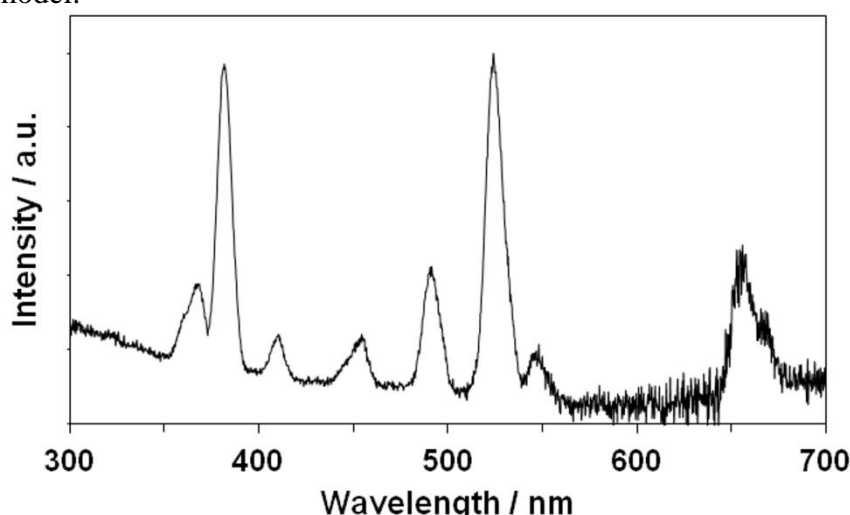


Figure S12. The excitation spectrum of complex **1** in liquid state monitored at 1540 nm.

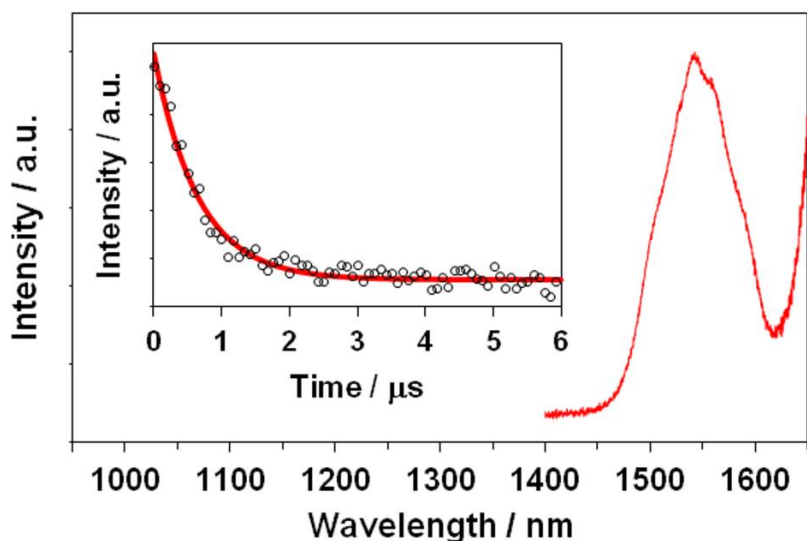


Figure S13. The emission spectrum of complex **1** in liquid state excited at 524 nm. The corresponding decay curve is in the inset. The solid curve is a monoexponential fitting.

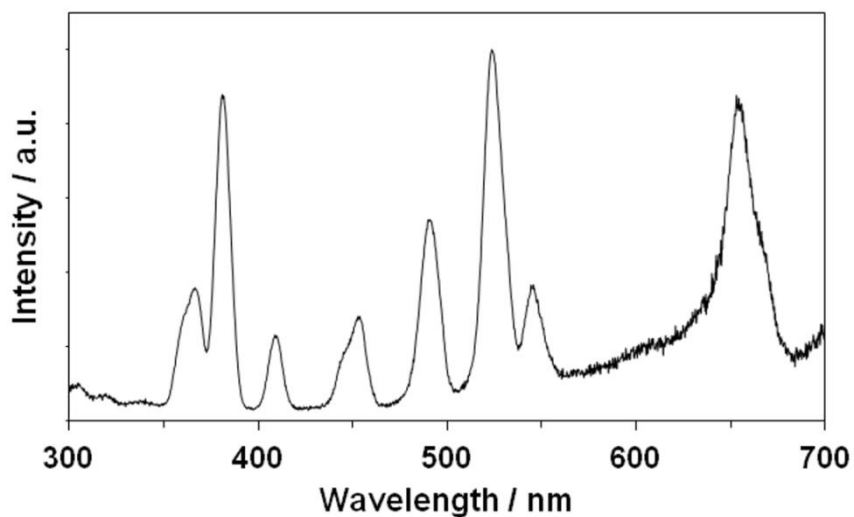


Figure S14. The excitation spectrum of complex **1** in solid state monitored at 1542 nm.

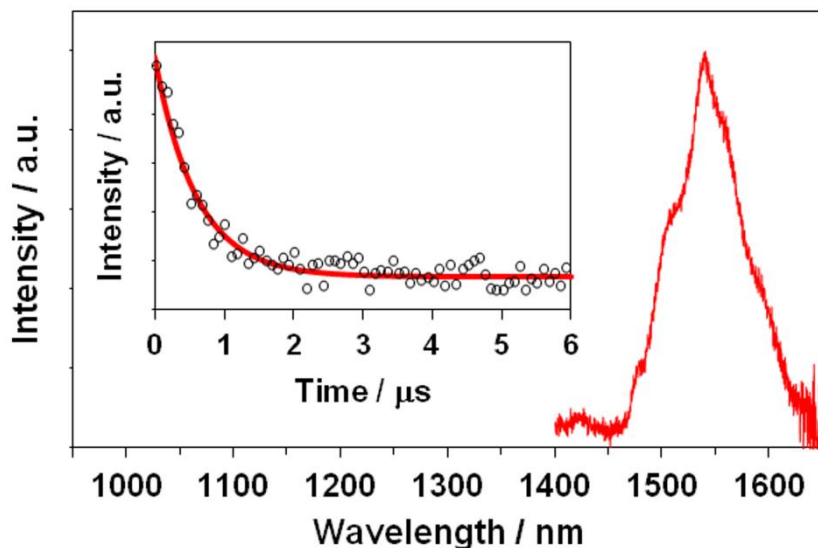


Figure S15. The emission spectrum of complex **1** in solid state excited at 524 nm. The corresponding decay curve is in the inset. The solid curve is a monoexponential fitting.

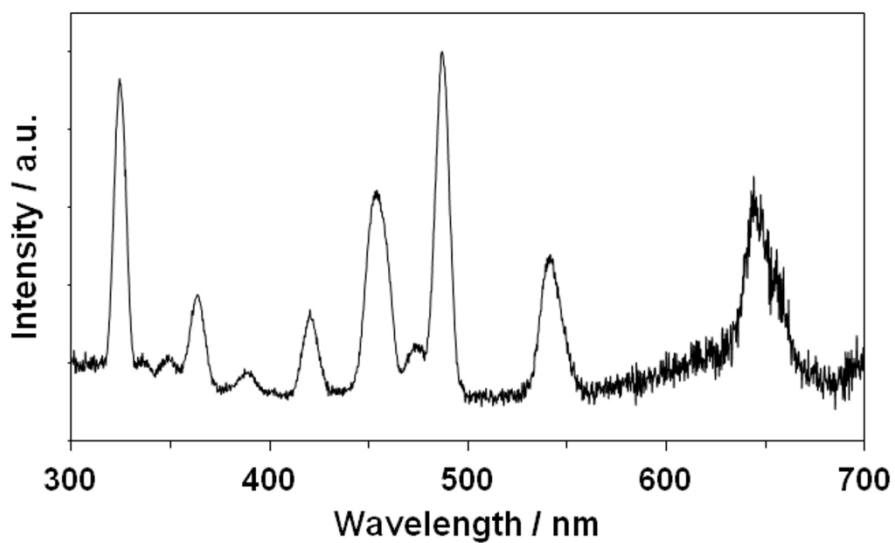


Figure S16. The excitation spectrum of complex **2** in liquid state monitored at 980 nm.

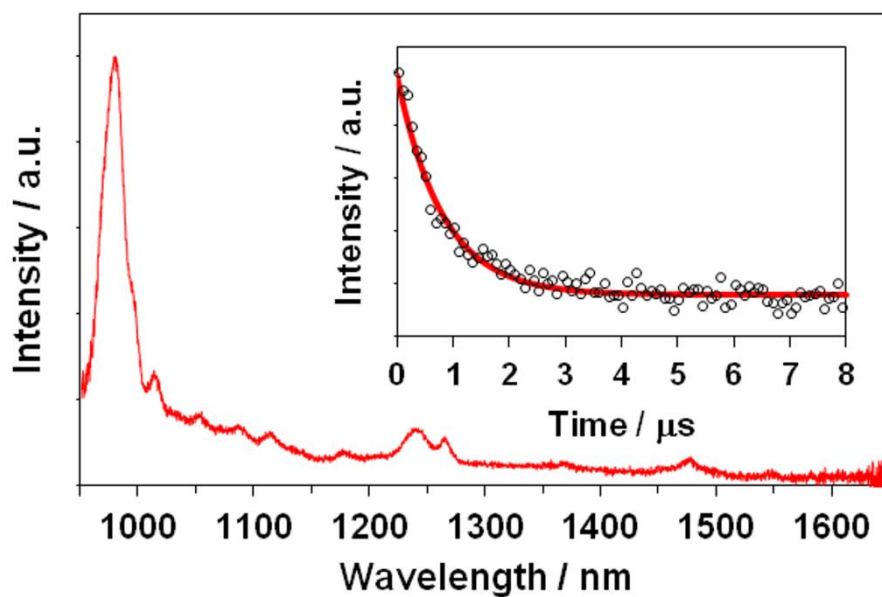


Figure S17. The emission spectrum of complex **2** in liquid state excited at 487 nm. The corresponding decay curve is in the inset. The solid curve is a monoexponential fitting.